PACS numbers: 42.65.Hw; 42.70.Ce; 42.81.Cn
DOI: 10.1070/QE2000v030n06ABEH001755

Spectral dependence of photorefractive effect in nitrogen-doped silica

O V Butov, K M Golant, A L Tomashuk

Abstract. Photoinduced variations in the refractive index of nitrogen-doped silica are directly measured in the wavelength range from 350 to 2500 nm. It is found that the change in the refractive index under the action of 193 nm laser radiation significantly increases in the long-wavelength region and amounts to $\sim 10^{-3}$ at $\lambda = 2.5$ μm (for the energy fluence $\sim 10^4$ J cm^{-2}). This means that the nature of the photorefractive effect in nitrogen-doped silica is related to photostructural transformations affecting the phonon part of the optical absorption spectrum.

By the photorefractive effect, it is commonly meant a change in the refractive index of a dielectric material under the action of optical radiation, as a rule laser radiation, whose intensity is lower than the destruction threshold of the material. In photorefractive crystals (e.g., sillenites), such refractive index changes are caused by the electro-optical effect. The latter is associated with the emergence of a volume-charge field due to photoinduced redistribution of electrons or holes trapped in the crystal (e.g., see Ref. [1]). The volume charge appears upon nonuniform irradiation of a crystal, which is accompanied by excitation, diffusion, and subsequent capture of itinerant photoelectrons at traps. This effect is reversible and is directly related to charge carrier generation as well as to charge transfer in a crystal.

A photorefractive effect of another kind is observed in some doped silica glasses. It represents a photoinduced change in the refractive index, which virtually does not relax to the initial state after irradiation. This effect occurs under UV laser irradiation, the magnitude of the effect being dependent on the radiation dose density (fluence), rather than on the incident radiation intensity. A glass is considered as being photosensitive, provided its refractive index increases by $10^{-4} - 10^{-3}$ at a fluence of $\sim 10 - 100$ kJ cm^{-2}.

Using such a glass, photoinduced in-fibre refractive index Bragg gratings can be fabricated (e.g. see Ref. [2]). The reflectivity of in-fibre Bragg gratings at the resonant wavelength is very high, whereas it is almost zero in the rest of the spectrum. Refractive index gratings are widely used in fibre optics as optical filters, fibre laser mirrors, and as sensing elements in sensors of physical quantities.

O V Butov, K M Golant, A L Tomashuk Fibre Optics Research Centre, General Physics Institute, Russian Academy of Sciences, ul. Vavilova 38, 117756 Moscow, Russia

Received 17 December 1999
Kvantovaya Elektronika **30** (6) 517 – 519 (2000)
Translated by A L Tomashuk, edited by M N Sapozhnikov

Among photosensitive glasses, germanosilicate glass occupies a prominent place, being the material of standard telecommunication fibres. The photorefractive effect in germanosilicate glasses is thought to be related to intra-centre excitation of the valence electrons of oxygen vacancies associated with germanium atoms. It is possible that a photo-induced local phase transition takes place [3], which results in an increase in the glass density in the vicinity of the vacancy and in an increase in the electron polarisability due to partial delocalisation of one of the two valence electrons of the oxygen vacancy [4]. Both delocalization of an electron and the increase in the glass density can lead to a refractive index change in a quantitative agreement with experiment.

Much less is known about the mechanism of the photorefractive effect in nitrogen-doped silica, which is a new photosensitive material for fibre optics [5]. An interesting and practically important feature of this glass is the capacity of Bragg gratings written in N-doped silica fibres to withstand heating up to 800 – 900 °C, whereas similar gratings written in germanosilicate fibres already decay at 400 – 500 °C [6].

Unlike germanosilicate glass, photorefractive effect occurs in N-doped silica only under the action of hard UV radiation at 193 nm. However, the energy of such a quantum is insufficient for the interband generation of charge carriers via single-photon absorption, because the energy gap of SiO_2 is ~ 9 eV. Optical absorption at $\lambda = 193$ nm is most likely to be related to the intracentre electronic transitions between the levels of nitrogen atoms, which are the main impurity centres, optically active in the UV region, similar to oxygen vacancies in germanosilicate glass. It is the photostructural transformations of a glass in the vicinity of these centres that appear to determine the photorefractive effect in N-doped silica. An important question is, however, which of the components of the polarisability of a medium is affected by the photostructural transformations: the electron polarisability caused by the displacement of valence electrons or the ion polarisability related to the displacement of atoms in the glass network.

To answer the above question, we have investigated the spectrum of the photorefractive effect. The aim was to determine the region in the transparency window of silica glass where the induced refractive index is larger. If the main changes occur in the short-wavelength spectral region adjacent to the fundamental interband absorption edge, then photoinduced changes in the electron component of polarisability play the key role. If the photoinduced refractive index changes prevail in the long-wavelength region adjacent to the fundamental bands of lattice (network) absorption, then the ion component of polarisability is more significant. These

propositions immediately follow from the Kramers – Kronig relations [7].

We measured chromatic dispersion of the glass refractive index before and after UV irradiation. Bulk glass samples in the form of a prism shown in Fig. 1 were used in the experiments. Between the central region of the prism and its cladding consisting of undoped silica, an N-doped silica core was situated. The prisms were produced from optical fibre preforms by cutting and polishing the lateral sides of the preforms in such a way that the prism edge coincided with the preform centre.

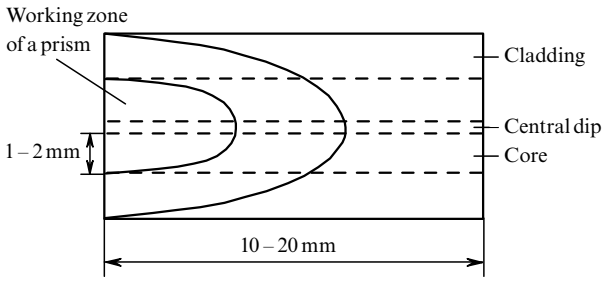

Figure 1. Lateral view of a prism used in the experiments.

The prism structure was dictated by the preform fabrication technology, which consisted of two stages [8]. First, an N-doped silica layer, about 300 μm in thickness, was formed on the inner surface of a substrate silica tube by the plasma-chemical vapour deposition process. Then, the tube with the deposited layer was heated by a torch until it softened and collapsed into a rod. At this stage, a considerable loss of nitrogen from the glass layer adjacent to the inner surface took place owing to nitrogen diffusion. As the result, the preform had a central dip in the radial distribution of nitrogen.

The optical schematic of the experimental setup is shown in Fig. 2. The method of transmission of a polychromatic light beam through a prism was used. Light from a white light source passed through two diaphragms and a prism, which was fixed on a rotating micropositioner, and then was focused by a lens on the entrance slit of a monochromator. The measurements were performed on a prism region composed of N-doped silica, which was separated by the second diaphragm. The signal of a photodetector placed behind the exit slit of the monochromator was detected with a standard synchronous detection scheme and then was fed to a computer. This scheme allowed us to determine the refractive index n to an accuracy of 2×10^{-4} in the spectral range between 350 and 2500 nm. The noise scatter of n values did not exceed

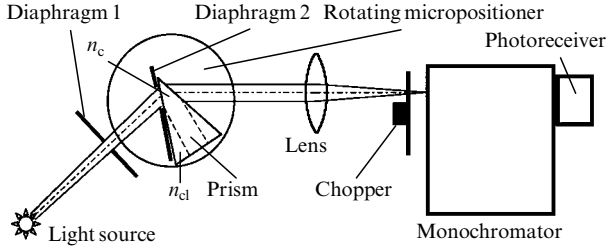

Figure 2. Optical schematic of the experimental setup (n_c and n_{cl} are the refractive indices of the core and the cladding).

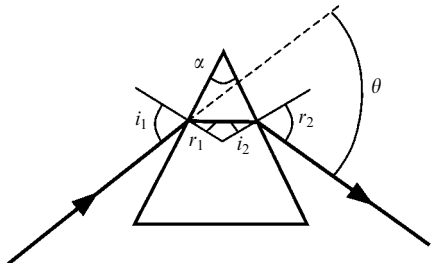

Figure 3. Light dispersion in a prism [9].

10^{-4}. The absolute experimental error was primarily due to the error in measuring angles i_1 and r_2 (Fig. 3) and divergence of the beam incident on the sample.

The refractive index dispersion was determined from the dependence of the prism rotation angle, corresponding to the maximal photoreceiver signal, on the wavelength. The measuring procedure was as follows. For each wavelength set by the monochromator, a prism rotation angle was determined that corresponded to the maximal photodetector signal. The wavelength step was 25 – 50 nm. The measuring procedure was fully automated. The refractive index was calculated numerically from relations

$$r_1 = \arcsin \frac{\sin i_1}{n}, \quad i_2 = |r_1 - \alpha| = \arcsin \frac{\sin r_2}{n},$$

$$\theta = i_1 - (r_1 + i_2) + r_2 = i_1 - \alpha + r_2 . \qquad (1)$$

Angles i_1, r_1, i_2, r_2, α, θ are shown in Fig. 3. Measured were angles i_1, r_2, and α, whereas angles θ and α remained unchanged, as is seen from Fig. 2.

The spectrum of the photorefractive effect was determined as the difference of dependences $n(\lambda)$ obtained on a prism before and after UV irradiation. We investigated two samples with approximately the same nitrogen atom content of ~ 3 %. Each of the two prisms was irradiated on both sides consecutively by the excimer ArF laser pulses, the pulse duration and repetition rate being 20 ns and 10 Hz, respectively. For the first sample, the total dose density amounted to 10 kJ cm^{-2}, with an average energy density per pulse of 290 mJ cm^{-2}, and for the second sample, 14 kJ cm^{-2}, with an average energy density per pulse of 210 mJ cm^{-2}.

Fig. 4 shows the dispersion curves obtained for the second sample before and after irradiation. Several independent measurements were performed for each wavelength, which allowed a reduction of the random error. The curves were approximated with the three-term Sellmeier formula (see, e.g., Ref. [10]):

$$n^2(\lambda) = 1 + \sum_{i=1}^{3} \frac{a_i \lambda^2}{\lambda^2 - b_i^2}, \qquad (2)$$

where a_i and b_i are constants.

Fig. 4 also shows the difference of the two dispersion curves (the right ordinate axis), i.e., the photorefractive effect spectrum. Dots are the values obtained by direct subtraction of $n(\lambda)$ measured before and after the UV irradiation. Almost identical curves were also obtained for the first sample.

One can see from Fig. 4 that the induced refractive index increases with the wavelength and reaches 10^{-3} at $\lambda \sim 2.5$ μm. In the UV region, on the contrary, the photorefractive effect is virtually absent. Note, however, that the induced refractive

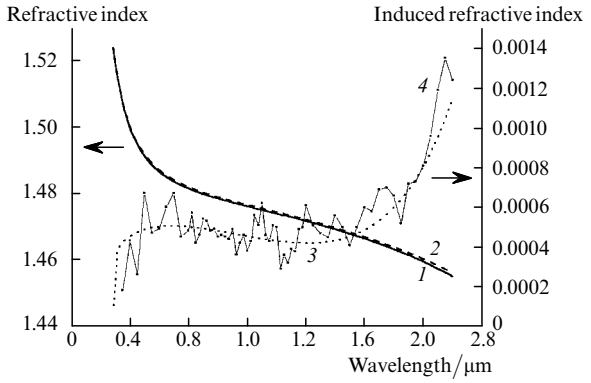

Figure 4. Refractive index dispersion in N-doped silica before and after UV irradiation: (1, 2) dispersion before and after irradiation approximated with the Sellmeier polynomial; (3) difference between curves 1 and 2; (4) difference between the experimental values before and after irradiation.

index increases nonmonotonically with the wavelength. This suggests that photoinduced changes occur also in the UV absorption spectrum. The UV absorption do not contribute significantly to the refractive index increase but affect the shape of the photorefractive effect spectrum.

The above results allow us to conclude that the main contribution to the photorefractive effect is made by sufficiently strong spectral changes in the phonon absorption region. These changes may be caused by optical densification of a glass under the action of radiation or by other photoinduced transformations affecting the IR absorption spectrum. The nature and mechanism of such transformations call for further investigation. In any case, it is clear that the photorefractive effect in nitrogen-doped silica is practically unrelated to changes in the electron component of high-frequency susceptibility.

Acknowledgements. This work was supported in part by the Russian Foundation for Basic Research (project No. 98-02-16361) and by RFBR-INTAS project No. IR-97-0877.

References

1. Grachev A I Fiz. Tverd. Tela **41** 1012 (1999) [Physics of the Solid State **41** 922 (1999)]
2. Russell P, Archambauit J. Phys. World (10) 41 (1993)
3. Tugushev V V, Golant K M J. Non-Crystal. Sol. **241** 166 (1998)
4. Golant K M, Tugushev V V Fiz. Tverd. Tela **41** 1019 (1999) [Physics of the Solid State **41** 928 (1999)]
5. Dianov E M, Golant K M, Khrapko R R, et al. Opt. Mater. **5** 169 (1996)
6. Dianov E M, Golant K M, Khrapko R R, et al. Electron. Lett. **33** 236 (1997)
7. Landau L D, Lifshitz E M Electrodynamics of Continuous Media (Moscow: Nauka, 1982)
8. Dianov E M, Golant K M, Kurkov A S, et al. J. Lightwave Technol. **13** 1471 (1995)
9. Lebedeva V V Eksperimental'naya Optika (Moscow: Izdatel'stvo MGU, 1994)
10. Fleming J W Appl. Optics **23** 4486 (1984)